Design and Practical Validation of a Hybrid Absorption/Compression Chiller Driven by Low-Grade Heat

Martin Helm, Thomas Eckert, Christian Schweigler

CENERGIE Competence Center Energieeffiziente Gebäude und Quartiere
Munich University of Applied Sciences, Lothstraße 34, 80335 Munich, Germany

Abstract

For all applications of sorption chillers or heat pumps strict limits have to be met, arising from the physical properties of the working fluids. A minimum temperature of the driving heat source has to be provided and the temperature lift of the cycle is limited. As a consequence, the chiller has to be oversized for application in solar cooling or tri-generation systems in order to adapt for low-grade driving heat. Due to the limited temperature lift of the working pair water as refrigerant and lithium bromide as sorbens the use of dry cooling towers is not feasible and in heat pumps systems only moderate heating supply temperatures can be provided.

When a mechanical compressor is integrated in the internal cycle of a sorption chiller, flexibility is obtained for a more compact and cost-efficient design and for adaptation to challenging operating conditions.

Design and first experimental results of a hybrid absorption/compression cycle are presented. An electrically driven high-speed turbo compressor is directly integrated in the sorption process of a single-stage water/LiBr cycle providing a variable share of the required pressure rise between evaporator and condenser. The system shall be operable in pure sorption mode and in hybrid absorption/compression mode, offering a boost of cooling capacity or increased flexibility for operation with low-grade driving heat or increased temperature of heat rejection.

Keywords: absorption chiller, vapor compression, hybrid cycle, turbo compressor, low-grade heat, temperature lift

1. Introduction

In the field of thermally driven cooling by absorption chillers based on the working pair water/lithium bromide substantial improvements have been achieved during the last decades concerning compactness, reliability, system performance and overall efficiency. But still, limitations in temperature lift due to the danger of crystallization of the sorbent solution, high required driving temperature and weak peak load capability at raised ambient temperatures narrow their field of application. To overcome these problems, the conventional absorption cycle can be equipped with a mechanical vapor compressor, forming a hybrid absorption/compression chiller. The basic concept has been theoretically described by (Osenbrück, 1895) and (Altenkrich, 1954), but not realized for water lithium bromide absorption chillers

The concept for realization of the hybrid absorption/compression cycle with an electrically driven high speed turbo compressor which is directly integrated in the single-stage absorption cycle is presented in (Helm, et al., 2015). The development of the hybrid chiller aims at 15 kW chilled water capacity at 6 °C chilled water temperature applying very low driving heat temperatures below 80 °C with dry heat rejection under European climate and high load change ability.

By means of a semi-empirical physical model, a preliminary design of the turbo compressor for the refrigerant water has been developed. Starting from this basic geometric layout, a 3D CFD fluid-dynamic and structural modeling of impeller and diffusor has been performed, using the software packages CF turbo and ANSYS-CFX. For the given conditions, the use of the refrigerant water results in high circumferential impeller velocities with vapor Mach numbers near the sonic barrier and rotational speed up to 90.000 rpm (Eckert, et al., 2016)

doi:10.18086/eurosun2018.04.20 Available at http://proceedings.ises.org

These design conditions and boundaries are fulfilled by a recently commercially available innovative turbo-compressor for the natural refrigerant water (R718). As core component, its performance has been experimentally investigated by detailed measurements throughout the entire operating envelope, in order to validate the perspectives of the hybrid chiller concept in advance to the implementation of the entire cycle.

Based on the promising results and practicality tests, a demonstrator of the hybrid chiller has been designed, erected and tested under different operating scenarios.

The overall goal of the development aims at reduced direct and indirect emissions of greenhouse gases for refrigeration by utilization of climate-neutral refrigerants and a high share of renewable or waste heat.

2. Concept of the hybrid absorption/compression chiller

In conventional sorption cooling or heat pump systems, a definitive interdependence of the three external temperature levels of the cycle, i.e. provision of cooling, heat rejection to ambient, and driving heat of the cycle, exists. This statement is valid, regardless whether a liquid or a solid sorbent is applied. As a consequence limitations arise for the implementation of chillers and heat pumps. The main aspect is the required temperature level of the driving heat source. In case of the liquid sorbent water/Lithium bromide a second constraint is given by the maximum allowed concentration of the sorbent solution, avoiding crystallization of the solution. In order to cope with the resulting limitation of the temperature lift, for standard cooling applications wet cooling towers have to be applied in order to provide sufficiently low cooling water temperatures.

In general, two system concepts for a single stage hybrid absorption & compression cycle are available (Eckert, et al., 2015). In the so-called EVA configuration the high speed turbo vapor compressor is integrated between Evaporator (E1) and Absorber (A1). In the DECO concept the compressor is arranged between Desorber (D1) and Condenser (C1).

In Figure 1 flow schemes for both cycle options are shown. The main components are qualitatively arranged according to the respective operating conditions. In analogy to the so-called Raoult plot, equilibrium temperature and pressure can be read from abscissa and ordinate, respectively. The representation is similar to the Dühring plot, where equilibrium temperature and dew point of the fluids are represented by abscissa and ordinate. Evaporator and condenser are aligned to the vapor pressure line of the refrigerant water. Between absorber and desorber sorbent solution is circulated in dilute and concentrated state. The two connecting lines follow the inclination of the respective isosteres in the Raoult plot.

In EVA configuration the absorber pressure is increased with reference to the evaporator, whereas in DECO mode the pressure lift of the compressor is found between desorber and condenser. As a consequence, for constant operating temperatures of the four main components, in EVA configuration the solution loop between absorber and desorber operates at lower LiBr concentration as compared to the DECO concept.

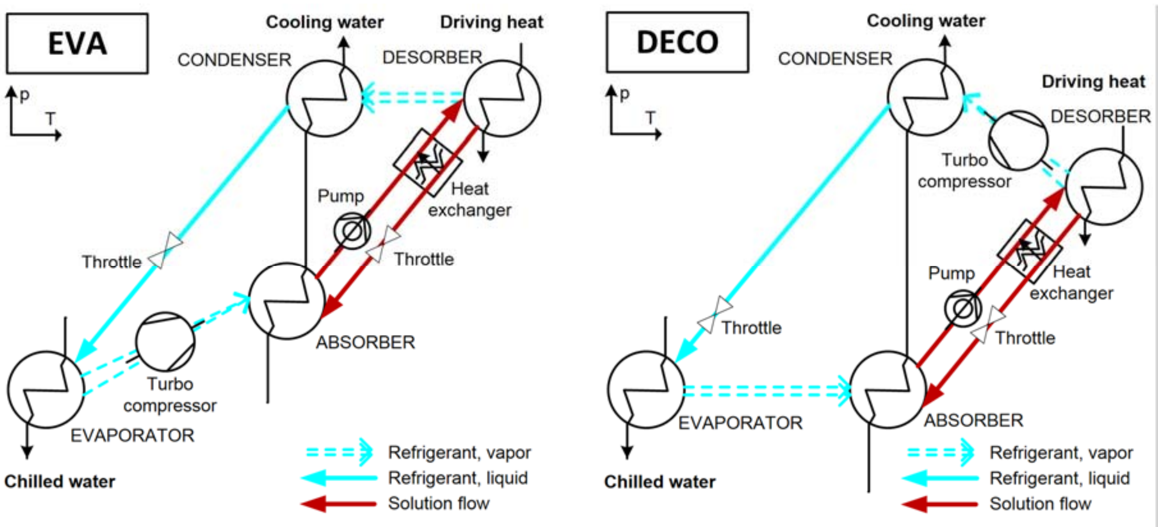

Figure 1: Scheme of the hybrid cycle with integration of the compressor between evaporator and absorber (EVA configuration) or desorber and condenser (DECO configuration).

The hybrid configuration of the absorption/compression cycle can be applied for different objectives, as shown in Figure 2, again based on the Raoult plot. As a reference, the single stage sorption cycle (Sorption) is shown represented by a rhomb formed by the two pressure levels of the evaporator/absorber pair and the condenser/desorber pair and the vapor pressure lines of the refrigerant water and the sorbent solution. Blue arrows indicate the driving temperature difference between the internal process and the external heat sources at desorber and evaporator and the heat sink at absorber and condenser.

For a given situation of chilled water and cooling water, the mechanical compressor serves for a reduction (Δt_2) of the operating temperature of the desorber. Consequently, driving heat of lower temperature is sufficient for operation of the chiller. This effect is accomplished by both concepts EVA and DECO, without general difference, as shown in Figure 2, left column. Although the temperature level of the driving heat is lowered, the capacity of the chiller remains constant, as expressed by the unchanged driving temperature differences.

The mechanical compressor can also be applied for boosting the capacity during operation with constant external temperatures, as shown in Figure 2, right column, center (Booster). Here the pressure lift of the compressor allows for higher pressure of condensation and lower pressure of evaporation in comparison to the standard sorption cycle. As a result, larger temperature differences for the heat transfer at all main components of the cycle are available, resulting in an increase of the capacity. This effect can be applied for cooling or heat pump applications.

The third major motivation for the integration of the mechanical compressor is the increase of the temperature lift (Δt_1) between the cooling effect provided by the evaporator and the heat rejection from absorber and condenser, as described by Figure 2, right column, bottom (High Lift).

Here "Booster" and "High Lift" are shown in EVA configuration. Of course, both effects can also be accomplished by application of the DECO concept.

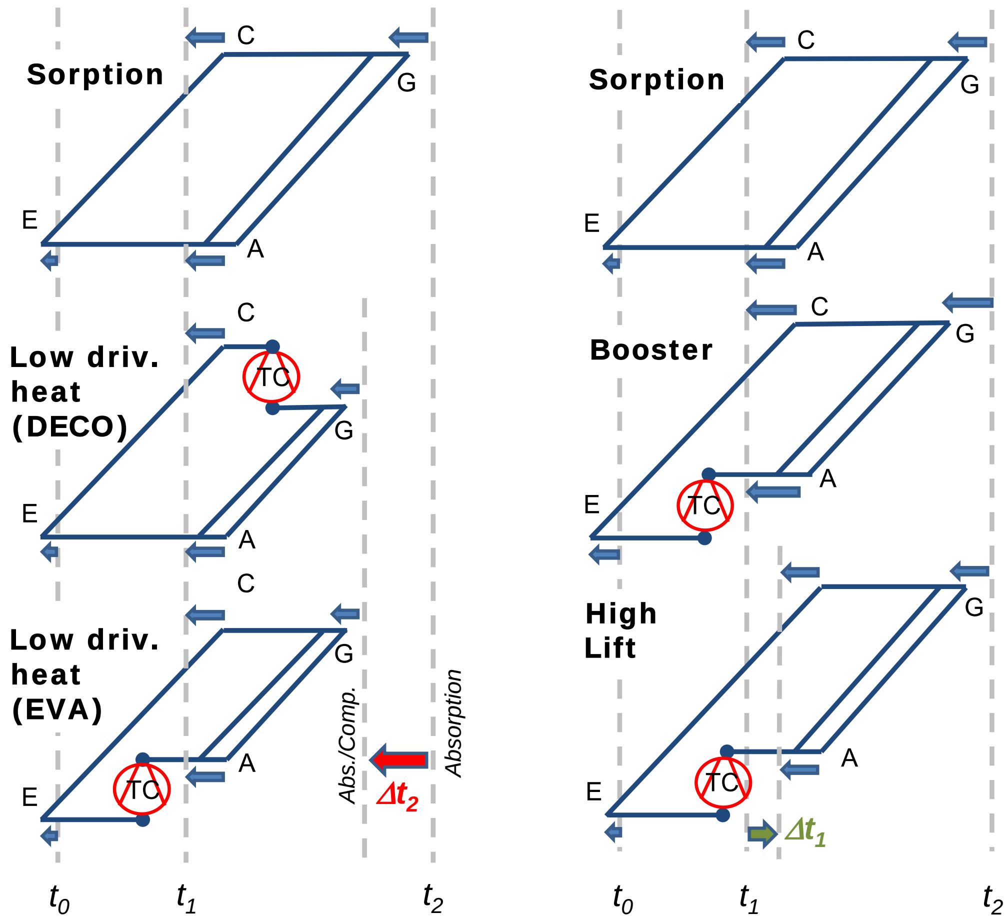

Figure 2: Effect of the mechanical compressor for adaptation of the hybrid sorption/compression cycle to low driving heat (EVA and DECO configuration, left) and for increase of capacity (right, center) or temperature lift (right, bottom)

3. Simulation of the hybrid absorption/compression chiller

A process model of the combined hybrid chiller has been set up by means of equation solver EES Academic Professional V10.268-3D. For the selected design with horizontal falling film tube bundles, preliminary studies showed heat transfer coefficients u in $kW \cdot m^{-2} \cdot K^{-1}$ of absorption (0.6), condensation (2.5) evaporation (1.2), desorption (0.6) and solution heat exchanger (1.0). In the following, both configurations of a hybrid sorption/compression chiller are simulated for compression ratios Π from 1 to 3 with an isentropic efficiency η variation of the compressor between 0.6 and 1.0 in order to evaluate process improvements in different operation scenarios. Dependent on the compression ratio Π and suction pressure at equilibrium temperature of the refrigerant T_{vle_ref}, a certain additional temperature lift ΔT_{lift} is provided to the sorption process. The additional temperature lift serves for improvement of the figures of merit given on the left ordinate of the diagrams shown in the following sections. The specific compressor rating P_{spec} represents the consumed electricity with regard to the refrigerating capacity, including flash losses due to the expansion to evaporator equilibrium. The solution flow rate is optimized for each run to obtain maximum efficiency and desired effect.

3.1 Increased cooling water temperature

Figure 3 shows the simulation results for increased cooling water inlet temperatures T_{cool} for EVA (left) and DECO (right) configuration. Exemplarily, a compression ratio Π of 2.5 at equilibrium suction temperature T_{vle_ref} = 5.5 °C (resp. 30 °C) adds additional ΔT_{lift} of 14.0 K (resp. 16.8 K) to the sorption process. The difference in ΔT_{lift} is caused by the Clausius–Clapeyron dependency of equilibrium temperature and pressure.

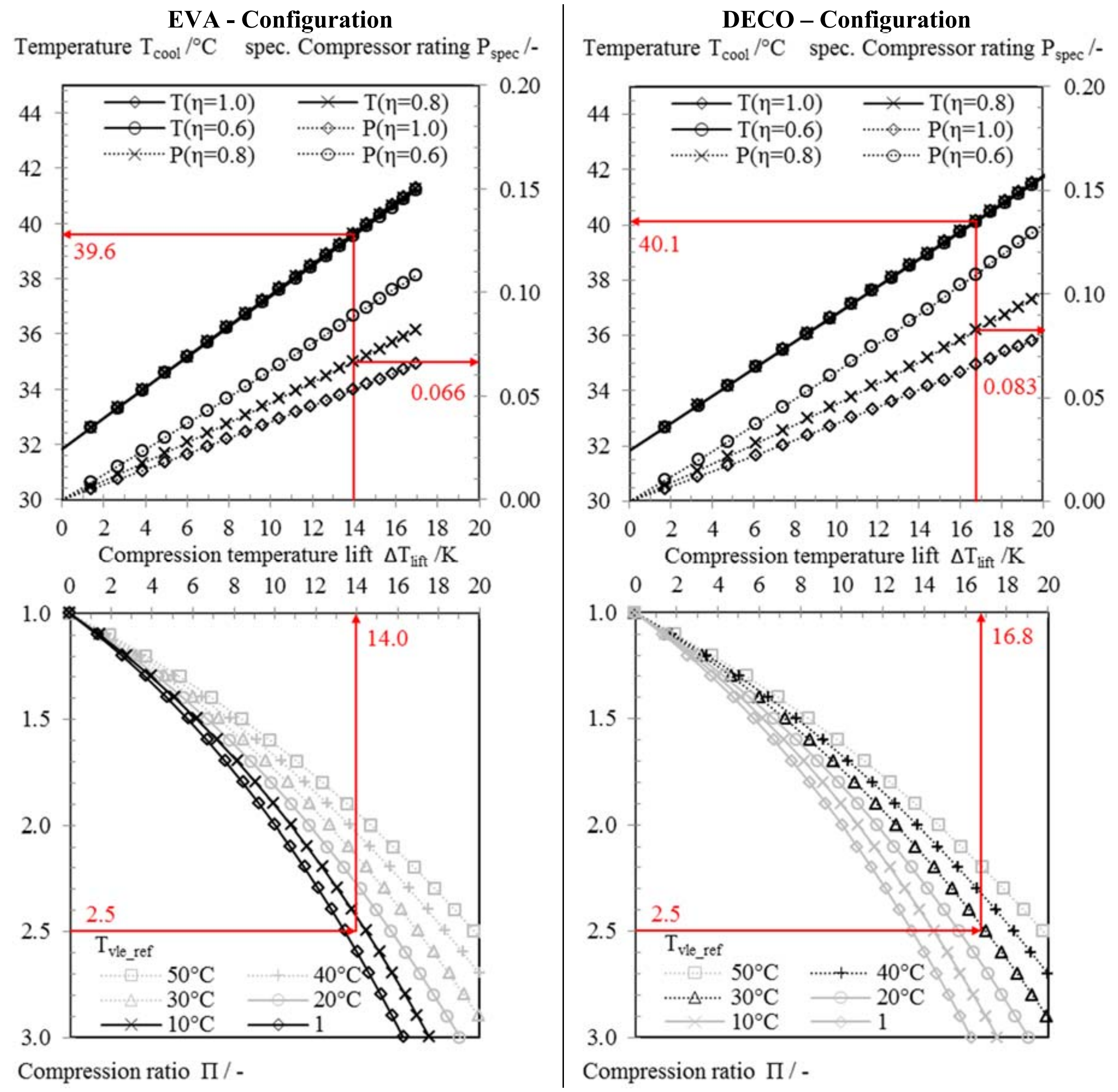

Figure 3: Process improvement map for increased cooling water temperatures.

With constant chilled water outlet temperature of 6 °C and driving heat inlet temperature of 80 °C the cooling water inlet temperature T_{cool} rises from formerly 32 °C to 39,6 °C (resp. 40.1 °C) at steady refrigerating capacity. This simplifies the dissipation of reject heat to the ambient and even allows the use of dry air coolers. While a decrease in the isentropic efficiency of the compressor η has only a minor effect on the attainable temperature level, the related specific auxiliary energy consumption P_{spec} increases reciprocally proportional.

3.2 Reduced driving heat temperature

When high reject heat temperatures of 40 °C and more are mandatory, driving heat inlet temperatures T_{heat} of almost 100 °C are required to provide a chilled water temperature of 6 °C. Besides the impendence of crystallisation, this exacts high requirements to system design, reduces efficiency and even prevents the use of absorption technology for some low temperature waste heat applications (e.g. use of heat from CHP-units or solar thermal systems).

Figure 4 depicts the effect on the required driving heat inlet temperature T_{heat} when a turbo-compressor operates with a compression ratio Π of 2.5 at corresponding vapour/liquid refrigerant equilibrium temperature at the compressor inlet T_{vle_ref} =5.5 °C and 30 °C in EVA and DECO-configuration respectively. As already observed in the previous operation mode, the isentropic efficiency has again a minor effect on the temperature level. As before, the DECO-configuration shows with T_{heat}=79.7 °C slightly better results than EVA with 80.9 °C, but converts the additional temperature lift less effectively. The specific auxiliary energy consumption ratio amounts to 0.0036 (EVA) and 0.0042 (DECO) Watts of electricity per Watt refrigerating capacity and Kelvin.

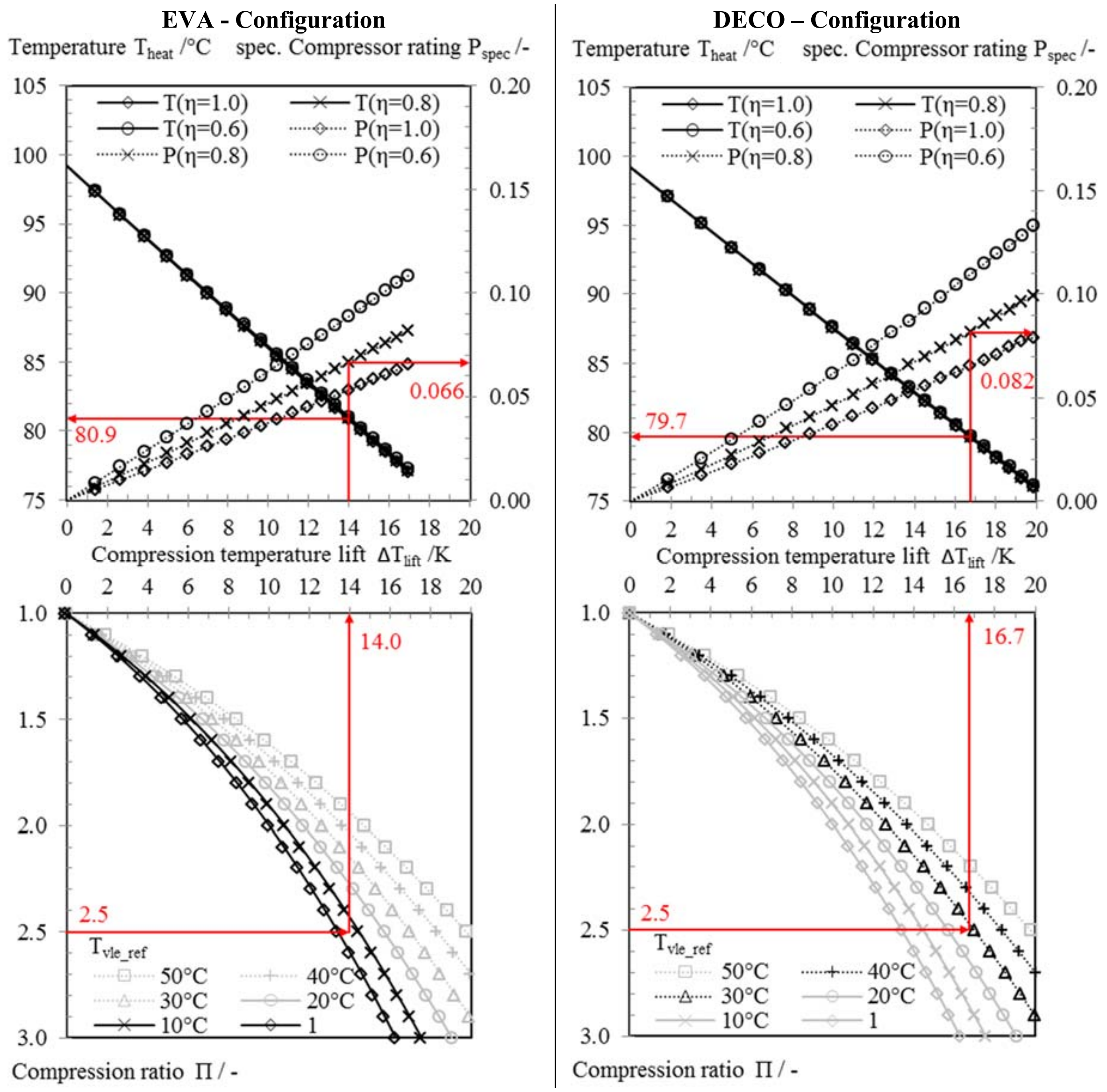

Figure 4: Process improvement map for reduced driving heat temperature.

Altogether, the turbo-compressor significantly reduces the required driving heat temperature level at given boundary conditions by up to 20 K and more at constant chilled water capacity. Consequently, at given inlet temperature the driving heat return temperature can be reduced accordingly, which has been confirmed by additional simulation. Due to size limitations for this publication no explanatory figures are given.

3.3 Capacity booster

The overall heat exchanger surface area is the decisive factor for the investment costs of absorption chillers. Usually, the design is made for maximum capacity at unfavourable operating conditions. Thus, the machine is substantially oversized for most of the operating hours. Additionally, the sorption process parameters have to be adjusted according to the fluctuating chilled water capacity to maintain high efficiency over a wide load range. The integrated turbo-compressor offers improvement for both aspects.

Figure 5 shows a significant increase of chilled water capacity related to design capacity Q_{rel} up to 190 % depending on the compression ratio Π of the turbo-compressor. Thereby, the additional temperature lift ΔT_{lift} is allocated proportionally to all heat exchanger components of the chiller, resulting in an overall lower evaporating temperature. Thus, the exemplary compression temperature lift in EVA-configuration reaches 13.8 K only, compared to the previous simulations. Likewise, the isentropic compressor efficiency η mainly effects the specific compressor rating, rather than the relative chilled water capacity. Due to the superheated inlet conditions of the refrigerant vapour the DECO-configuration performs worse, again expressed by the higher specific compressor rating P_{spec}.

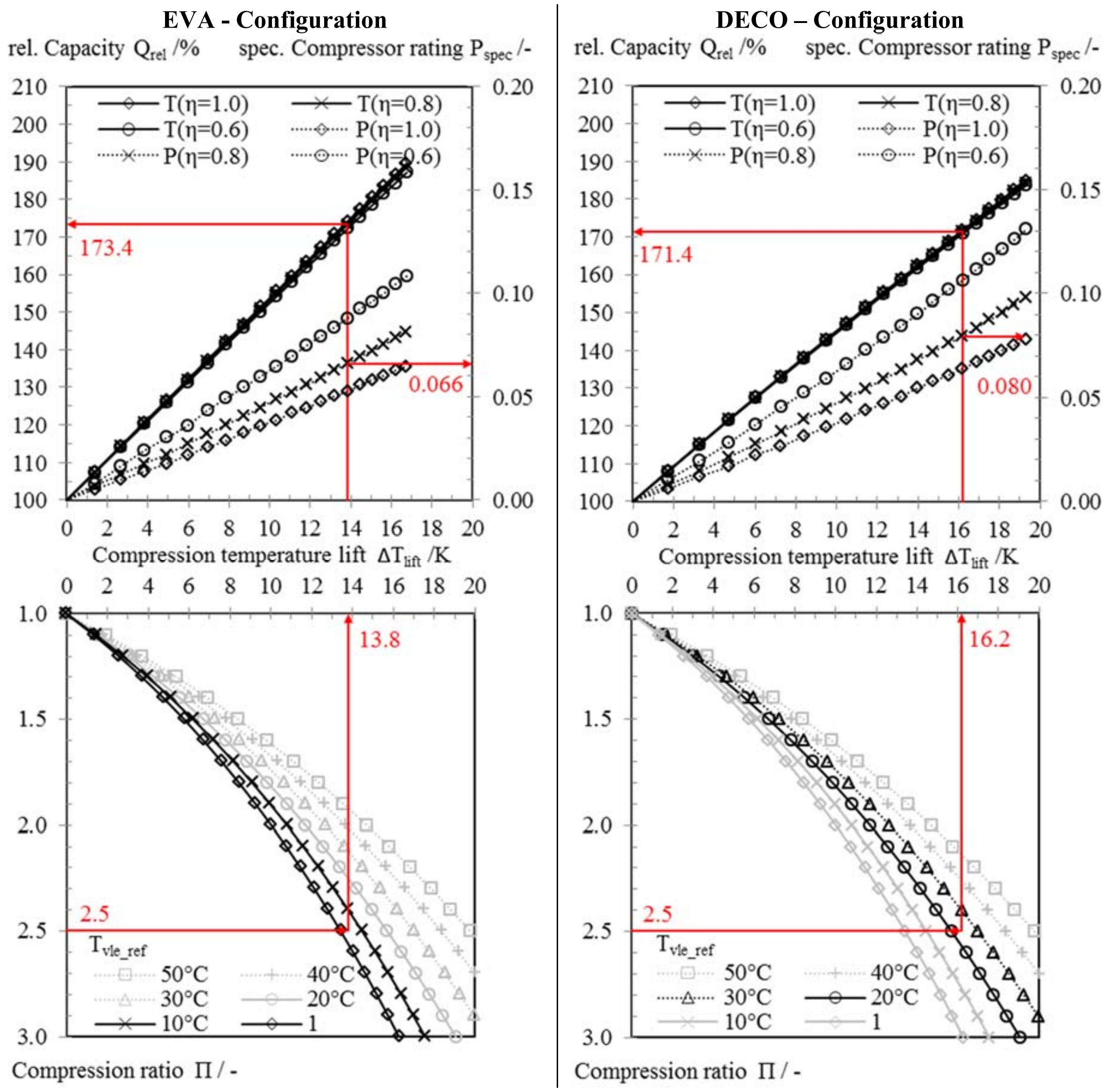

Figure 5: Process improvement map of capacity booster mode.

4. Hybrid chiller design studies and demonstrator setup

A laboratory test plant of the hybrid absorption/compression chiller has been designed and constructed which can be operated in pure absorption mode and hybrid operation with variable contribution of the mechanical compressor. The centrifugal compressor has been provided by a commercial partner who offers two-stage vapor compression chillers with the refrigerant water (Efficient energy GmbH, 2016) (Meier-Staude & Kniffler, 2013).

Due to its thermodynamic properties the natural refrigerant Water requires a revised absorption chiller design if a turbo compressor is integrated. In the refrigerant flow pressure losses have to be reduced to a minimum despite extremely high flow conditions near sonic velocity. In addition, entrainment of refrigerant droplets is to be avoided at the compressor inlet.

For the design of the chiller different geometric concepts have been set up and analyzed, as shown in Figure 6 (a) to (f). In all cases a circular or symmetric arrangement has been chosen. For the main components different types of heat exchanger structures are applied. In terms of a preliminary assessment the integration of the cylindrical compressor unit is shown for both pressure vessels, i.e. evaporator/absorber and desorber/condenser unit, respectively

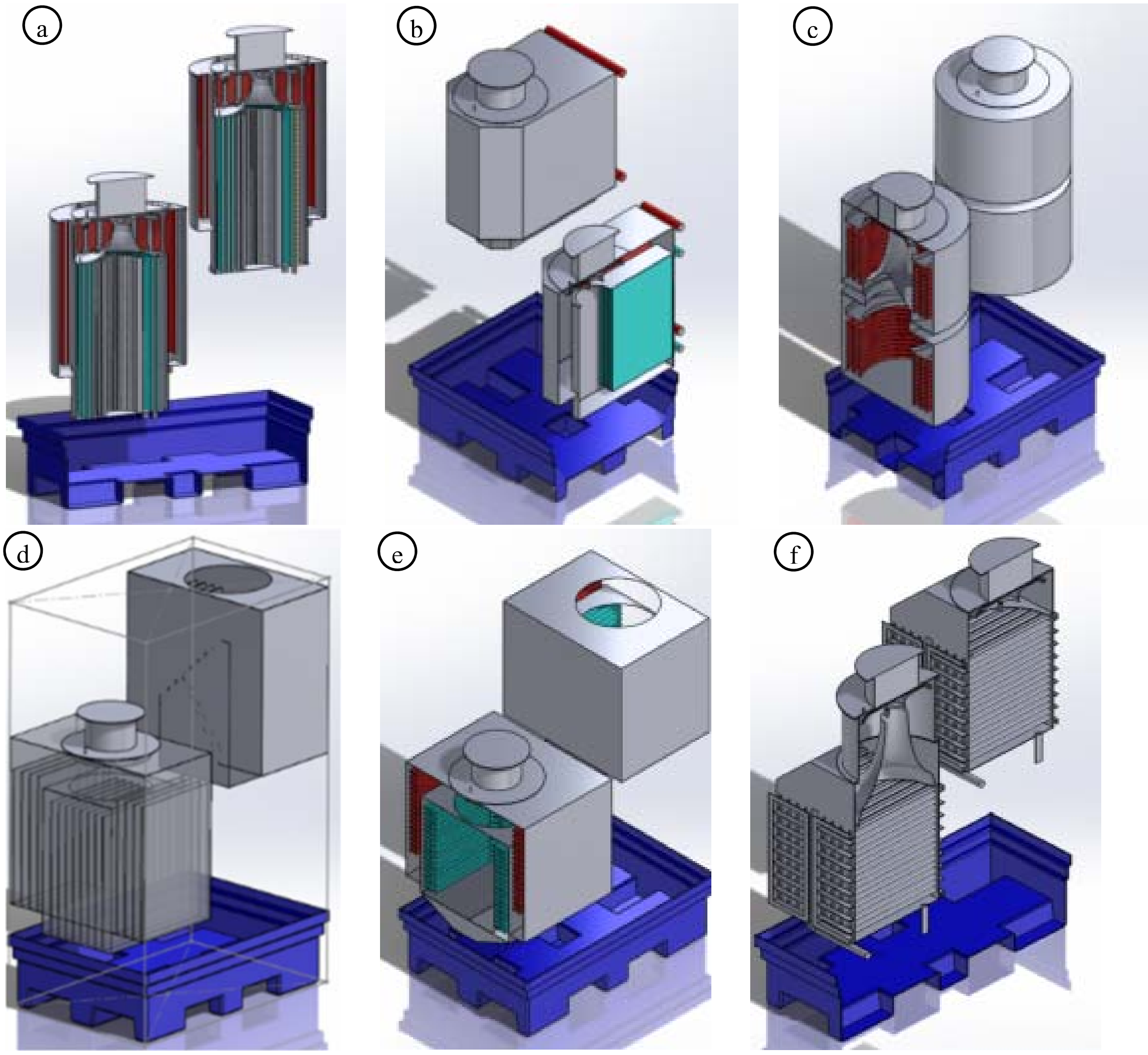

Figure 6: Design concepts for the hybrid chiller test plant; configurations (a) to (f) from top left to bottom right.

In design (a) concentric circular plates form the main component heat exchangers. This concept would offer a perfect match with the circular shape of the turbo compressor. Yet, for the compact dimensions of the commercial compressor circular plate heat exchangers with sufficiently small diameter are not available. In design (b) stacks of parallel thermoplates are used as heat exchangers. In the evaporator/absorber unit the evaporator is positioned in the center.

The absorber is arranged in two parts and surrounds the evaporator on both sides. A negative aspect is the reduced flow cross-section for the refrigerant vapor at the compressor inlet. Concentric helical tube coils are applied for concept (c). For the internal process this configuration offers similar conditions like a conventional tube bundle. Yet, due to the long tube length high pressure drops occur in the external heat carrier circuits. Design (d) is based on parallel packages of thermoplates. Here again high pressure drops in the refrigerant vapor flow have to be expected within the volume of the heat exchangers.

As a conclusion, resulting from the requirements of the refrigerant vapor flow decision has been taken for a conventional shell and tube design comprising horizontal tube bundles for the main component heat exchangers. In order to match the circular geometry of the compressor first u-shaped tube bundles as shown in design (e) have been taken into consideration. Yet, finally design (f) with classical horizontal tube bundles in parallel arrangement has been chosen in order to avoid complex geometric constructions.

Based on the above design study the test plant of the hybrid chiller has been designed resorting to the conventional falling film design of the main component heat exchangers evaporator, absorber, condenser and desorber. The two components operating at low pressure, and high pressure respectively, are arranged in a symmetric configuration with vapor flow from the central component through the compressor to the outer part of the vessel. In order to reach a symmetric geometry all main components have been split in two parts. In the low pressure part of the chiller the two evaporator sections are positioned in the center, separated by a void volume in which the released refrigerant vapor flow is directed upward to the compressor. The compressed vapor finally reaches the two absorber sections which are positioned in the outer parts of the vessel. Optionally, the compressor can be installed in the high pressure section of the cycle with vapor flow from the desorber to the condenser. Figure 6(f) shows a sectional view of the test plant with identical design of the low and high pressure vessel. The conic suction dome forming the compressor inlet is mounted on top of the lower vessel.

The test plant of the hybrid chiller has been erected and equipped like a conventional sorption chiller with all required auxiliary instrumentation and sensors for scientific measurement as shown in Figure 7. A purge system comprising a liquid/gas ejector and a scroll vacuum pump is applied for conservation of the vacuum. Operation of the internal pumps, concentration of the sorbent solution and anti-freeze control of the evaporator is handled by a compact PLC control unit. In order to assure stable operating conditions for the turbo compressor an anti-surge valve has been installed. The valve is equipped with a fast motor drive for opening a return line from the compressor discharge to the suction side of the compressor. By that means the refrigerant flow through the compressor can be maintained above the minimum allowed flow and the occurrence of surge is avoided.

For pure sorption mode of the hybrid chiller without contribution of the compressor bypass-flaps have been forseeen between evaporator and absorber compartment, similar to the design of conventional water/Silicagel adsorption chillers. During standstill of the compressor the refrigerant vapor passes through the self-acting flaps in addition to the flow path across the compressor. Thus, the pressure drop between evaporator and absorber is minimized.

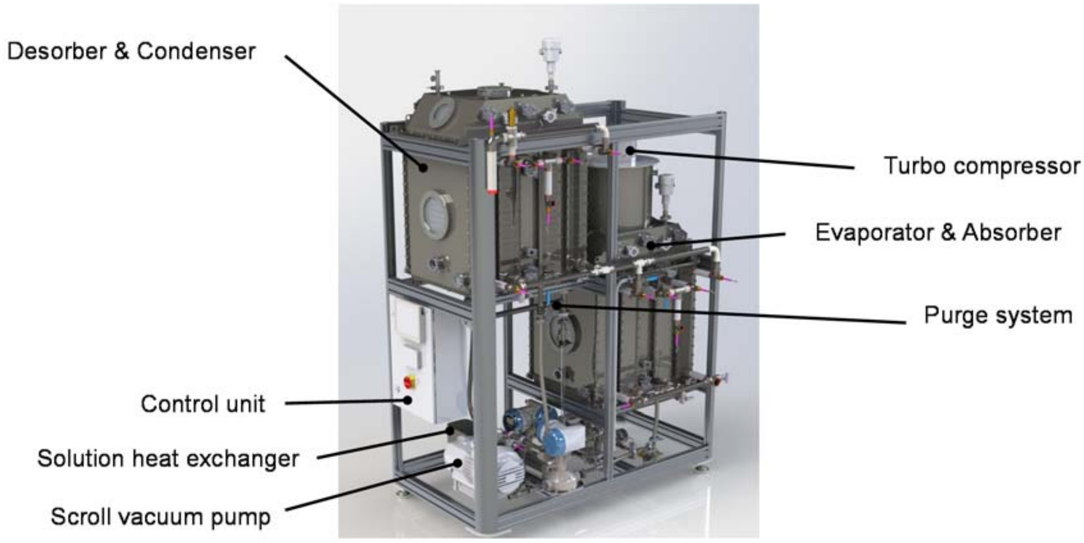

Figure 7:3D-CAD Model of the hybrid chiller demonstrator and main components

5. Practical validation of the hybrid chiller concept

Supported by the additional temperature lift provided by the compressor, the three different effects - increased temperature lift from chilled water supply to heat rejection / reduced temperature level of the driving heat / booster-mode with increased chilled water capacity at unchanged operating conditions – have been examined at a test-rig at Munich University of Applied Sciences.

The following tables show the main parameters - such as temperatures T, volume flow rates V and lithium bromide mass concentration w - in Evaporator (E1), Absorber (A1) and Desorber (D1) as well as the heat ratio ζ_C of the sorption process. Furthermore, the standard deviation of the sample σ during the entire measuring phase of 10 minutes for quasi-stationary evaluation conditions is given. Supportive figures allow a graphical comparison with the EVA simulation results of chapter 3.

Figure 8 depicts measuring results for increased cooling water inlet temperatures T_{cool} in relation to the simulation results, depending on the temperature lift ΔT_{lift} provided by the mechanical compressor in EVA-configuration. Additionally, the required specific compressor rating $P_{\_spec}$ is given.

Table 1: Parameters of the absorption-compression process for increased cooling water temperature mode.

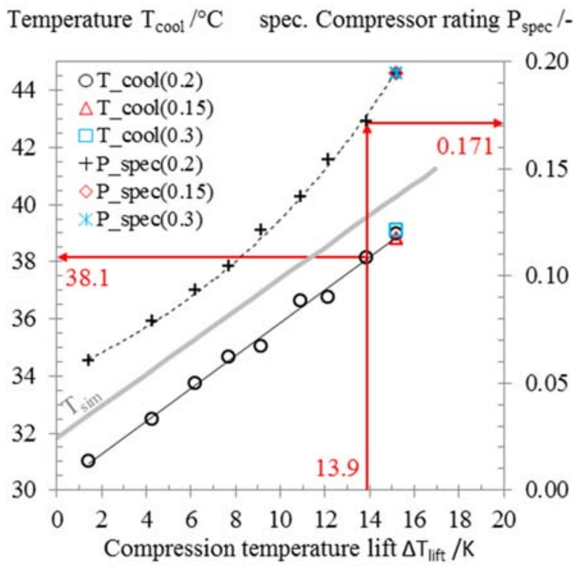

Parameter	Unit	Value	σ
E1#T_brine_IN	°C	12.1	$\pm 3.9 \times 10^{-2}$
E1#T_brine_OUT	°C	6.2	$\pm 2.9 \times 10^{-2}$
A1#T_cool_IN	°C	38.1	$\pm 9.4 \times 10^{-2}$
A1#V_cool	$m^3 \cdot h^{-1}$	3.6	$\pm 1.3 \times 10^{-2}$
A1#V_sol_OUT	$m^3 \cdot h^{-1}$	0.2	$\pm 1.0 \times 10^{-2}$
A1#w_sol_OUT	$\%_{mass}$	50.1	$\pm 1.7 \times 10^{-2}$
D1#T_heat_IN	°C	79.5	$\pm 1.1 \times 10^{-1}$
D1#T_heat_OUT	°C	71.8	$\pm 8.8 \times 10^{-2}$
D1#w_sol_OUT	$\%_{mass}$	53.0	$\pm 1.9 \times 10^{-2}$
P_{spec}	-	0.171	$\pm 8.2 \times 10^{-3}$
ζ_C	-	0.793	$\pm 1.3 \times 10^{-2}$

Figure 8: Effect of the temperature lift ΔT_{lift} ,provided by the mechanical vapor compressor, on required cooling water inlet temperature T_{cool} and specific compressor rating P_{spec} with H_2O/LiBr-solution flow rates of 0.15, 0.2 and 0.3 $m^3 \cdot h^{-1}$.

A variation of the lithium bromide solution flow rate from 0.15 to 0.3 $m^3 \cdot h^{-1}$ shows no significant effect on the examined parameters. The coefficient of determination R^2 reaches 0.9933 % (linear) for T_cool and 0.9989 % (2nd order polynomial) for P_{spec}. A deviation of about -1.8 K between measured and simulated results – represented as bold grey line – is observed and can be mainly attributed to irreversibilities and losses of the test-rig. For an exemplary temperature lift ΔT_{lift} = 13.9 K the cooling water inlet temperature increases from formerly 30 °C to 38.1 °C. In that case, the required specific compressor rating amounts to P_{spec} = 0.171 and an overall sorption process heat ratio ζ_C of 0.793 is achieved. The effect for the operating temperature is in good agreement with the theoretic model as discussed in section 3. Yet, the electric power demand strongly exceeds the predictions due to the low efficiency of the electric drive of the compressor. Unfortunately, a measurement of the shaft power for more detailed analysis of the fluid mechanic performance has not been available.

As summarized in Table 1, the hybrid chiller provides 6.2 °C of chilled water (E1#T_brine_OUT), at a cooling water inlet temperature A1#T_cool_IN = 38.1 °C with a driving heat temperature of D1#T_heat_IN = 79.5 °C at the desorber inlet. Meanwhile, the maximum lithium bromide concentration remains at a moderate value of D1#w_sol_OUT = 53.0 $\%_{mass,}$ which has a positive effect on heat and mass transfer coefficients and reduces corrosion potential. Nevertheless, the conversion factor between ΔT_{lift} and the gain in T_{cool} is lower than 1 due to the sorption process. This may lead to the conclusion, that an external coupling of sorption and compression cycle might be more effective. Yet, this advantage may be missed if large temperature differences in the external heat transfer circuits occur.

Figure 9 shows the measured driving heat temperature level T_{heat} in comparison to the simulation results, which are represented as bold grey line, in dependency of the mechanical compression temperature lift T_{lift}. Additionally, the specific compressor rating P_{spec} needed to decrease the driving heat inlet temperature is given. The coefficient of determination R^2 reaches 0.925 % (linear) for T_{heat} and 0,9975 % (2nd polynomial) for P_{spec}.

Table 2 summarizes the indicative parameters of the hybrid chiller process for an exemplary mechanical temperature lift T_{lift}=13.7, which causes a specific compressor rating P_{spec} of 0.169, defined as units of electricity per unit cooling (external chilled water capacity plus internal refrigerant expansion losses). As a result, the required driving heat inlet temperature level decreases from formerly almost 100 ° to 84.1°°C for a chilled water outlet temperature E1#T_brine_OUT of 6.0 °C and a cooling water inlet temperature to the absorber of A1#T_cool_IN=39.9 °C. Meanwhile the cooling water flowrate remains constant at A1#V_cool=3.6 $m^3 \cdot h^{-1}$. With a solution flowrate A1#V_sol_OUT=0.2 $m^3 \cdot h^{-1}$ between Absorber (A1) and Desorber (D1) the lithium bromide concentration w varies between 51.3 and 54.7 $\%_{mass}$. Without the mechanical compressor at given external temperature levels a much higher driving heat temperature would be required, leading to risky lithium bromide concentrations of 62 % and more, which might result in crystallisation and eventually failure of the chiller. Despite the high temperature difference between chilled and cooling water, the heat ratio of the sorption process ζ_C=0.778 is quite good. Very advantageous is the high conversion factor between ΔT_{lift} and T_{heat}. In this case, the mechanical compressor adds 13.7 K temperature lift to the internal sorption process, which results in a decrease of the driving heat inlet temperature of more than 15 K.

Table 2: Parameters of the absorption-compression process for decreased driving heat temperature mode.

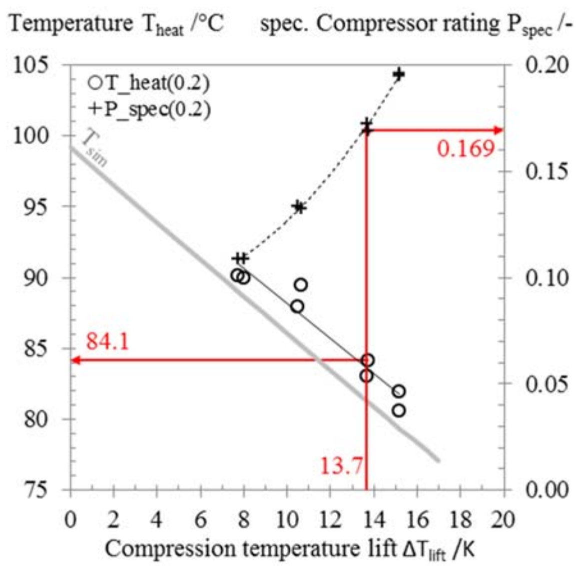

Parameter	Unit	Value	σ
E1#T_brine_IN	°C	12.0	$\pm 3.1 \times 10^{-2}$
E1#T_brine_OUT	°C	6.0	$\pm 2.5 \times 10^{-2}$
A1#T_cool_IN	°C	39.9	$\pm 9.4 \times 10^{-2}$
A1#V_cool	$m^3 \cdot h^{-1}$	3.6	$\pm 2.2 \times 10^{-2}$
A1#V_sol_OUT	$m^3 \cdot h^{-1}$	0.2	$\pm 1.0 \times 10^{-2}$
A1#w_sol_OUT	$\%_{mass}$	51.3	$\pm 1.4 \times 10^{-2}$
D1#T_heat_IN	°C	84.1	$\pm 1.1 \times 10^{-1}$
D1#T_heat_OUT	°C	76.3	$\pm 6.3 \times 10^{-2}$
D1#w_sol_OUT	$\%_{mass}$	54.7	$\pm 2.3 \times 10^{-1}$
P_{spec}	-	0.169	$\pm 4.5 \times 10^{-3}$
ζ_C	-	0.778	$\pm 1.1 \times 10^{-2}$

Figure 9: Effect of the temperature lift ΔT_{lift}, by means of mechanical vapour compression, on the required driving heat temperature T_{heat} and therefore spent specific compressor rating P_{spec} at aqueous lithium bromide solution flow rate of 0.2 $m^3 \cdot h^{-1}$.

Figure 10 presents the additional chilled water capacity Q_{add} when a mechanical vapor compressor provides a certain temperature lift ΔT_{lift} between Evaporator and Absorber. Furthermore, the corresponding compressor rating P_{spec} is shown. The tests have been carried out with cooling water inlet temperatures of 30, 35 and 40 °C. In contrast to the simulation figures, the increase in chilled water capacity is depicted in absolute values as the reference cooling capacity for each set of cooling water inlet temperature variation deviates.

The most relevant measuring results are listed in Table 3 for an exemplary hybrid chiller test with A1#T_cool_IN=34.9 °C cooling water inlet temperature at constant flowrate A1#V_cool=3.6 $m^3 \cdot h^{-1}$ and compression temperature lift ΔT_{lift}=12.9 K. By means of a specific compressor rating of P_{spec}=0.154 the chilled water capacity increases about +6.7 kW. The coefficient of determination R^2 at cooling water inlet temperatures 30, 35 resp. 40 °C reaches 0.997, 0.992 resp. 0.9863% (linear) for the additional capacity Q_{add} and 0.997, 0.9989 resp. 0.9071 % (2nd order polynomial) for the specific compressor rating P_{spec}. While the compressor rating at 35 °C cooling water is in good accordance with the simulation results the other two test runs show contradictory curve shape. This can be explained by the characteristic operation map of the turbo-compressor which has been modelled with constant efficiency.

Under given boundary conditions the refrigerant flow rate through the compressor is quite high and therefore close to the choke limit with reduced compression efficiency. Furthermore, flow losses gain increasing importance. Both effects result in an increase of P_{spec} at rising ΔT_{lift}. In contrast to this, a higher cooling water temperature of 40 ° shifts the operation point of the turbo-compressor towards its surge limit, again at reduced efficiency. In addition, chilled water capacity is quite low, resulting in an unfavourable operational state of the compressor due to its poor base load performance. Again, both aspects induce an increase of P_{spec} at reduced ΔT_{lift}.

Table 3: Parameters of the absorption-compression process for improved chilled water capacity mode.

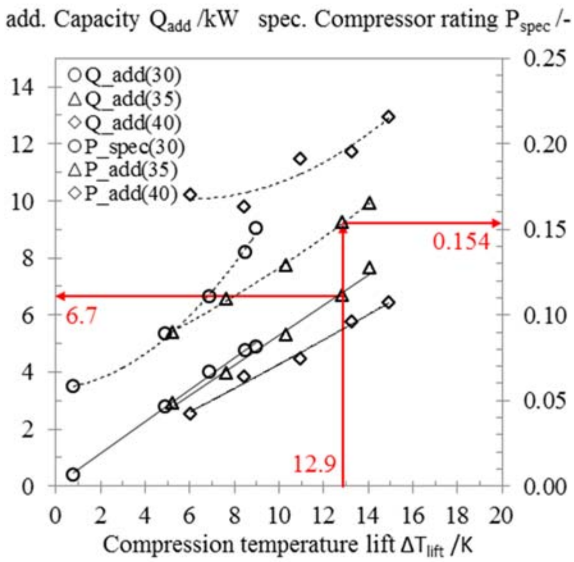

Parameter	Unit	Value	σ
E1#T_brine_IN	°C	12.1	$\pm 2.1 \times 10^{-1}$
E1#T_brine_OUT	°C	6.1	$\pm 1.0 \times 10^{-1}$
A1#T_cool_IN	°C	34.9	$\pm 1.8 \times 10^{-1}$
A1#V_cool	$m^3 \cdot h^{-1}$	3.6	$\pm 2.1 \times 10^{-2}$
A1#V_sol_OUT	$m^3 \cdot h^{-1}$	0.2	$\pm 1.0 \times 10^{-2}$
A1#w_sol_OUT	$\%_{mass}$	50.1	$\pm 2.6 \times 10^{-2}$
D1#T_heat_IN	°C	80.1	$\pm 1.7 \times 10^{-1}$
D1#T_heat_OUT	°C	70.6	$\pm 9.4 \times 10^{-2}$
D1#w_sol_OUT	$\%_{mass}$	54.1	$\pm 2.8 \times 10^{-1}$
P_{spec}	-	0.154	$\pm 4.8 \times 10^{-3}$
ζ_C	-	0.803	$\pm 3.4 \times 10^{-2}$

Figure 10: Additional chilled water capacity Q_{add} depending on additional temperature lift ΔT_{lift} from the mechanical vapour compression and therefore spent specific compressor rating P_{spec} at cooling water inlet temperatures 30, 35 and 40 °C.

6. Summary and Outlook

A hybrid chiller concept based on the natural refrigerant water R718 and consisting of an adapted lithium bromide absorption machine with directly integrated mechanical vapor turbo compressor with variable compression ratio Π between 1 and 3 is introduced. Considering conventional design parameters, two constructive combinations are possible in general. The EVA-configuration contains the turbo compressor between Evaporator and Absorber of the sorption process, while in the DECO-configuration it's arranged between Desorber and Condenser.

A steady-state simulation of both hybrid absorption/compression process configurations shows several positive effects on the system behavior under varying boundary conditions for solar cooling applications. For instance, with increasing additional compressor input higher cooling water inlet temperatures up to +10 K are possible or the required driving heat temperature level decreases by up to 20 K. In another case, if all external temperature levels remain constant, the compressor input directly boosts the chilled water capacity to almost 190 % of the design value. Based on the promising results, a hybrid chiller demonstrator with conventional horizontal tube falling film heat exchangers and 15 kW chilled water capacity has been designed, built and tested at Munich University of Applied Sciences laboratories. The thermal results are in good accordance with the simulation for all evaluated operation modes. Yet, rather poor values have been obtained for the effective auxiliary energy consumption, as the power train of the mechanical compressor is not optimized for the given conditions. Thus, due to the lack of a shaft power measurement the energetic effect of the hybrid cycle concept could not be fully evaluated.

Further investigations focus on an effective implementation of the examined operational modes in order to optimize the seasonal performance and investment costs of the hybrid chiller for promising applications such as solar cooling, tri-generation systems and district heating networks.

Acknowledgement

This project is funded by the German ministry of Education and Research under grant number 13FH023I3

7. References

Altenkrich, E., 1954. *Absorptionskältemaschinen.* Berlin: Verl. Technik.

Eckert, T., Helm, M., Schweigler, C., 2015. *Lithium bromide / R718 Hybrid Soprtion & Compression Cycle,* Yokohama, Japan: 24th IIR International Congress of Refrigeration (ICR2015), Congress Proceedings. doi: 10.18462/iir.icr.2015.0560.

Eckert, T., Helm, M. & Schweigler, C., 2016. *Design of a centrifugal Turbo Compressor with the working fluid water for the operation in a hybrid sorption/compression heat pump cycle.* Seoul, Korea, ASME Turbo Expo. doi:10.1115/GT2016-58177.

Efficient energy GmbH, 2016. *Technical data eChiller 2-35,* Feldkirchen, Germany.

Helm, M., Eckert, T. & Schweigler, C., 2015. *Hybrid Water/LiBr Absorption chiller boosted by high-speed turbo compressor,* Rome, Italy: 6th International Conference Solar Air-Conditioning.

Meier-Staude, R. & Kniffler, O., 2013. *Entwicklung und Herstellung von Prototypen der Verdampfer und Verflüssiger für die ct-turbo Wärmepumpe,* Feldkirchen: Efficient Energy GmbH.

Osenbrück, A., 1895. *Verfahren zur Kälteerzeugung bei Absorptionsmaschinen.* Germany: in Kaiserliches Patentamt.